PHYSICAL REVIEW D VOLUME 48, NUMBER 9 1 NOVEMBER 1993

Screening mass from chiral perturbation theory, virial expansion, and the lattice

V. L. Eletsky*
Institute for Theoretical Physics, Bern University, CH-3012 Bern, Switzerland

J. I. Kapusta
School of Physics and Astronomy, University of Minnesota, Minneapolis, Minnesota 55455

R. Venugopalan
Theoretical Physics Institute, University of Minnesota, Minneapolis, Minnesota 55455
(Received 28 May 1993)

We calculate the electric screening mass in hot hadronic matter using two different approaches, chiral perturbation theory and the relativistic virial expansion with empirical phase shifts, and compare the results to each other and to a gas of free pions and ρ mesons. We also compute the electric screening mass for noninteracting, charged bosons with mass m on a lattice to study likely finite-size effects in lattice gauge theory simulations of continuum QCD. For a lattice of given size, the continuum can be properly represented only for a window in the ratio T/m.

PACS number(s): 12.38.Mh, 12.38.Lg, 12.38.Gc

I. INTRODUCTION

The advent of a new generation of heavy ion accelerators is making it possible to produce hadronic matter at high temperatures and densities. Specifically, we refer to temperatures near the pion mass and densities greater than the density at the center of atomic nuclei. Little is known about the properties of these hot and dense systems and of their expected transition to a phase consisting of quarks and gluons. In principle, both of these phases are described by QCD, but the structure of this theory is especially complicated for the above-mentioned region of temperatures and densities. It is therefore reasonable to use a wide array of techniques to investigate different aspects of the behavior of hot and dense hadronic matter.

One way in which we can investigate the properties of this many-body system is to study its response to a small perturbation using linear response theory. This response can then be expressed in terms of correlation functions unperturbed by the presence of the probe. For example, we could ask for the response of an electrically neutral system to an applied, static, electric field. The system responds to a weak perturbation, such as a heavy, charged lepton or hadron, by dynamically Debye screening the long-range Coulomb force. The Debye screening length is independent of the external perturbation.

In Ref. [1] the inverse of the Debye screening length, the electric screening mass, $m_{\rm el}$, was studied in hot QCD. Interestingly, this can be done in two different ways. One way is to compute the photon self-energy. The electric screening mass squared is then the static, infrared limit of the time-time component of the self-energy. Another way is through an identity which relates the electric screening mass squared to the pressure

$$m_{\rm el}^2 = e^2 \left(\frac{\partial^2 P}{\partial \mu^2} \right)_{\mu=0} , \tag{1}$$

where μ is the electric charge chemical potential. Both ways of computing the screening mass are exact.

In this work, we will use Eq. (1) to calculate the electric screening mass for a hot pion gas. This is done using three very different techniques, namely, the relativistic virial expansion, chiral perturbation theory, and lattice theory, which are discussed in successive sections. In the virial approach, dynamical information obtained from empirical two-body scattering phase shifts is used to compute the pressure for an interacting pion gas with a nonzero chemical potential and hence, from Eq. (1), the electric screening mass. In the following section the screening mass is computed using finite temperature chiral perturbation theory, extended to the case of a nonzero chemical potential. The results of chiral perturbation theory are found to agree exactly with those of the virial expansion in the low temperature Boltzmann limit, $T \ll m_\pi$, to order $(T/m_\pi)^{3/2}$. Finally, we compute the screening mass for free, massive, bosons on a lattice. The ratio of the screening mass on the lattice to that in the continuum is studied parametrically as a function of T/m, where m is the mass of the boson. This gives an indication of how large a lattice is needed in order that lattice gauge theory properly approach the continuum QCD limit. See Fig. 1, taken from Ref. [1].

Each of the above-mentioned methods, as might be expected, has its advantages and disadvantages. The relativistic virial expansion demonstrates how the influence of both resonant and repulsive interactions may be in-

*On leave from Institute of Theoretical and Experimental Physics, Moscow 117259, Russia.

 ©1993 The American Physical Society

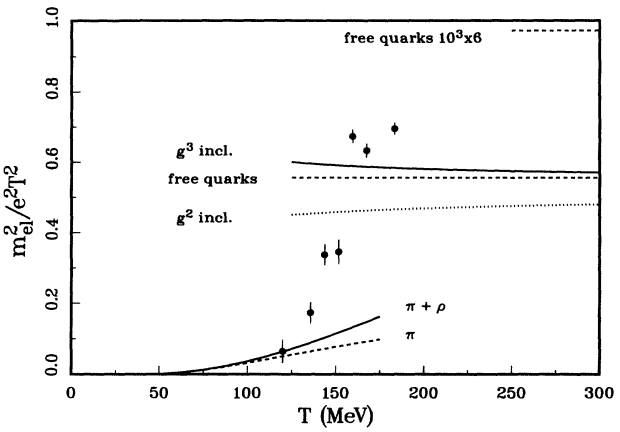

FIG. 1. The square of the electic mass in units of e^2T^2 vs temperature. At low T the two lines represent the contributions from pions, and pions plus ρ mesons. At high T the three lines represent the contributions from up and down quarks computed to the indicated order in the QCD coupling. The data points are from lattice QCD calculations on a $10^3 \times 6$ lattice. For free massless up and down quarks on a lattice of this size $m_{\rm el}^2/e^2T^2 = 35/36$ as indicated by the dashed line in the upper right-hand corner. In this figure the pion mass was taken to be one-half the ρ mass in order to facilitate comparison with the lattice results. Taken from Ref. [1].

cluded in calculations of the electric screening mass at temperatures close to the pion mass. Since the virial expansion can be expressed as an expansion in powers of the density, the results of this approach very likely contain the right physics for dilute systems. If, however, the system is dense, three- and higher-body interactions are significant. Extracting this information from the empirical phase shifts is difficult. The chiral perturbation theory approach is of interest since it contains many of the low energy properties of QCD. It also explains some of the low energy hadron phenomenology successfully. Furthermore, since the Lagrangian is known, many quantities of physical interest can be studied. A limitation of this approach, though, is that resonant interactions are not fully accounted for. These may be expected to contribute significantly for temperatures close to the pion mass. Currently, lattice gauge theory is a popular technique to understand the structure of strongly interacting matter. This includes studies of various correlation functions of mesons on the lattice. While lattice gauge theory is in principle very powerful, finite-size effects are important. Analytic calculations for free, massive, bosons on the lattice are therefore very useful in quantifying the sizes of these effects.

In addition to being of intrinsic physical interest, our calculation of the electric screening mass is also illustrative because these techniques may be used to compute dispersion relations and other response functions. The importance of alternative techniques to calculate various correlation functions has been discussed by Shuryak [2], who has used both experimental phase shifts as well as QCD sum-rule techniques to compute dispersion relations for hot hadronic matter [3]. In this way we may get a better physical understanding of the immense information that may in principle be available from both heavy ion experiments and future lattice gauge theory simulations, especially with the Teraflop project.

II. RELATIVISTIC VIRIAL EXPANSION

The relativistic virial expansion has been used recently to compute the thermodynamic properties of a dilute gas of interacting hadrons [4,5]. This approach is appealing because it allows one to systematically include the effects of both resonant and repulsive interactions in finite temperature hadronic matter by relating the state variables to the known, empirical, phase shifts. In this section we will use the relativistic virial expansion to compute the electric screening mass for a gas of interacting pions. It will be shown in the following section that the virial expansion results also provide an excellent check of chiral perturbation theory calculations with nonzero chemical potentials.

The relativistic virial expansion, introduced by Dashen and co-workers [6], relates thermodynamic state variables of a system of interacting particles to the S matrix. The partition function is separable into a product of the noninteracting partition function Z_0 and an interacting term which is proportional to bilinear products of the S matrix and its inverse. The logarithm of the partition function can be written as

$$\ln Z = \ln Z_0 + \sum_{i_1,i_2} z_1^{i_1} z_2^{i_2} b(i_1,i_2)\,, \tag{2}$$

where $z_j = \exp(\beta\mu_j)$ for $j = 1,2$ are the fugacities. The virial coefficients $b(i_1,i_2)$ are written as

$$b(i_1,i_2) = \frac{V}{4\pi i}\int \frac{d^3P}{(2\pi)^3}\int dE \exp\left[-\beta(P^2+E^2)^{1/2}\right] \times \mathrm{Tr}_{i_1,i_2}\left(AS^{-1}(E)\frac{\overleftrightarrow{\partial}}{\partial E}S(E)\right)_c\,. \tag{3}$$

In the above, the inverse temperature is denoted by β while V, P, and E stand for the volume, the total center-of-mass momentum, and energy, respectively. The labels i_1 and i_2 refer to a channel of the S matrix which has an initial state containing $i_1 + i_2$ particles—the trace is therefore over all combinations of particle number. The symbol A denotes the symmetrization (antisymmetrization) operator for a system of bosons (fermions) while the expression with the double-headed arrow is defined as

$$S^{-1}\left(\overleftrightarrow{\partial}/\partial E\right)S \equiv S^{-1}(\partial S/\partial E) - (\partial S^{-1}/\partial E)S\,. \tag{4}$$

The subscript c refers to the trace over all connected diagrams. The lowest virial coefficient $B_2 \equiv b(i_1,i_2)/V$ as $V \to \infty$ corresponds to the case where $i_1 = i_2 = 1$.

At temperatures close to the pion mass, the system is assumed to be sufficiently dilute for the hadrons to interact chiefly via elastic collisions. This assumption greatly simplifies Eq. (4) since the S matrix can be expressed in terms of the phase shifts δ_l^I as

$$S(E) = \sum_{l,I} (2l+1)(2I+1) \exp(2\delta_l^I) , \tag{5}$$

where l and I denote the angular momentum and isospin, respectively. The above assumption also implies that two-body interactions are dominant relative to the three-body and higher terms. The two-body interactions are expressed via the second virial coefficient

$$B_2 = \frac{1}{2\pi^3 \beta} \int_M^\infty dE\, E^2 K_2(\beta E) \sum_{l,I}{}' g_{l,I} \frac{\partial \delta_l^I(E)}{\partial E} . \tag{6}$$

The factor $g_{l,I} \equiv (2l+1)(2I+1)$ is the degeneracy of the (l, I) channel and M is the invariant mass of the interacting pair at threshold. The prime over the summation sign denotes that for given l the sum over I is restricted to values consistent with statistics. If the phase shifts $\delta_l^I \to 0$ as $E \to M$, an integration by parts yields

$$B_2 = \frac{1}{2\pi^3} \int_M^\infty dE\, E^2 K_1(\beta E) \sum_{l,I}{}' g_{l,I} \delta_l^I . \tag{7}$$

For further details on the behaviour of the virial coefficients and expressions for the thermodynamic state variables, we refer the reader to Ref. [5].

In the pion gas, the π^+, π^-, and π^0 have chemical potentials $+\mu$, $-\mu$, and zero, respectively. The chemical potential in Eq. (2), $\mu_1 + \mu_2 \equiv \mu_Q$, corresponds to the net conserved charge Q in each scattering channel contributing to Eq. (2). The $\pi\pi$ pressure due to interactions can then be expressed as

$$P_{\pi\pi}^{\rm int} = \sum_Q P_Q^{\rm int} , \qquad P_Q^{\rm int} = T e^{\beta \mu_Q} B_{2,Q} , \tag{8}$$

where for $-2 \le Q \le 2$, $-2\mu \le \mu_Q \le 2\mu$. The different $\pi\pi$ channels contributing to the second virial coefficient $B_{2,Q}$ for each Q can then be decomposed, with the appropriate Clebsch factors, into the corresponding spin-isospin channels. After a little algebra, the interacting $\pi\pi$ pressure in the above equation is finally written in terms of the spin-isospin phase shifts as

$$P_{\pi\pi}^{\rm int} = \frac{T}{2\pi^3} \int_{2m_\pi}^\infty dE\, E^2 K_1(\beta E) \left[2\cosh(2\mu\beta)\delta_0^2 + 2\cosh(\mu\beta)(\delta_0^2 + 3\delta_1^1) + \delta_0^2 + 3\delta_1^1 + \delta_0^0 \right] . \tag{9}$$

The total pion pressure is given by the sum of the above interacting pressure and the ideal gas pressure

$$P_\pi^{\rm ideal} = \frac{1}{6\pi^2} \int_0^\infty \frac{dp\, p^4}{\omega} \left[\frac{1}{e^{(\omega-\mu)/T} - 1} + \frac{1}{e^{(\omega+\mu)/T} - 1} + \frac{1}{e^{\omega/T} - 1} \right] . \tag{10}$$

The electric screening mass for the interacting pion gas can then be obtained from Eq. (1). We get

$$m_{\rm el}^2 = \frac{e^2 m_\pi^2}{\pi^2} \left[\sum_{n=1}^\infty K_2(\beta n m_\pi) + \frac{1}{m_\pi^2 \pi T} \int_{2m_\pi}^\infty dE E^2 K_1(\beta E) \left(5\delta_0^2 + 3\delta_1^1 \right) \right] . \tag{11}$$

The second term in the above equation is the contribution to the electric screening mass from the interactions. In Ref. [4] it was shown that the pressure of an interacting pion gas was nearly identical to the sum of the pressures of an ideal gas of pions and (Maxwellian) ρ mesons up to rather large values of the temperature. This was due to a near exact cancellation of the isospin weighted sum of the spin-zero phase shifts leaving only a contribution from the δ_1^1-resonant phase shift. Unlike the pressure, however, the screening mass for an interacting $\pi\pi$ gas is *not* the sum of the screening masses of an ideal gas of π and ρ mesons. In Fig. 2 we plot the electric screening mass squared (in units of e^2T^2) for an ideal gas of π's and ρ's as well as for an interacting pion gas using the expression in Eq. (11). They agree fairly well at lower temperatures but disagree by 10% or more at temperatures above the pion mass. The screening masses in the two cases differ because of the presence of a repulsive δ_0^2 piece in the interacting $\pi\pi$ screening mass in Eq. (11). In its absence, they would agree almost exactly for the temperatures considered.

In the above formulas, the virial expansion has been

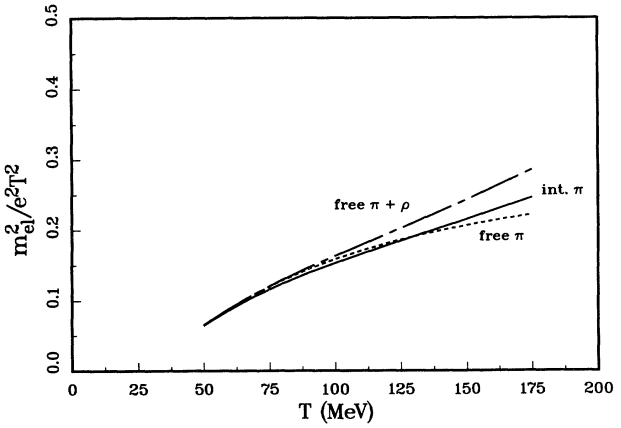

FIG. 2. Square of electric screening mass in units of e^2T^2 vs temperature. The dashed line is the contribution from a free gas of π mesons; the chain-dashed line includes free ρ mesons as well. The solid line is the square of the screening mass for an interacting pion gas computed using empirical $\pi\pi$ phase shifts in the relativistic virial expansion.

truncated at the level of the second virial coefficient; only two-body collisions were considered. At temperatures above the pion mass, three- and higher-body interactions will begin to contribute significantly. Since it is virtually hopeless to expect to obtain complete experimental data on the S matrix for m particles in and n particles out, the extension of this approach to high densities is limited. One would have to rely on models of the many-body interactions, as obtained from effective Lagrangians, for example.

III. CHIRAL PERTURBATION THEORY

In this section, we will use the method of effective chiral Lagrangians [7–9] to calculate the electrostatic screening mass in a pion gas at finite temperature. We will generalize the calculation of the pressure of a pion gas performed in Ref. [9] to the case of a finite chemical potential associated with electric charge and then obtain $m_{\rm el}^2$ using Eq. (1).

The partition function is given by a Euclidean functional integral

$$\mathrm{Tr}\,\exp(-H/T) = \int [dU] \exp\left(-\int_T d^4x L_{\rm eff}\right), \quad (12)$$

where $U(x) = \exp[i\phi^a(x)\tau^a/F]$ is an SU(2) matrix comprising the pion field $\phi(x)$. The integration should be performed over all configurations which are periodic in Euclidean time, $U(\mathbf{x}, x_4 + \beta) = U(\mathbf{x}, x_4)$. The effective Lagrangian $L_{\rm eff}$ is expressed as an infinite set of terms with increasing number of derivatives or quark masses,

$$L_{\rm eff} = L^{(2)} + L^{(4)} + L^{(6)} + \cdots . \quad (13)$$

The leading term corresponds to the nonlinear σ model:

$$L^{(2)} = \tfrac{1}{4}F^2 \mathrm{Tr}\left[\partial_\mu U^\dagger \partial_\mu U - m_0^2 (U + U^\dagger)\right] . \quad (14)$$

The coupling constant F is the pion decay constant in the chiral limit and m_0 is the pion mass in the lowest order in quark masses:

$$m_0^2 = -\frac{1}{2F^2}(m_u + m_d)\langle \bar{u}u + \bar{d}d\rangle . \quad (15)$$

Neglecting isospin breaking in the quark masses, the next order Lagrangian may be written in the form [9]

$$\begin{aligned} L^{(4)} = & -\frac{1}{4}l_1 \left[\mathrm{Tr}\left(\partial_\mu U^\dagger \partial_\mu U\right)\right]^2 \\ & -\frac{1}{4}l_2 \mathrm{Tr}\left(\partial_\mu U^\dagger \partial_\nu U\right) \mathrm{Tr}\left(\partial_\mu U^\dagger \partial_\nu U\right) \\ & +\frac{1}{8}l_4 m_0^2 \mathrm{Tr}\left(\partial_\mu U^\dagger \partial_\mu U\right) \mathrm{Tr}\left(U + U^\dagger\right) \\ & -\frac{1}{16}(l_3 + l_4) m_0^4 \left[\mathrm{Tr}(U + U^\dagger)\right]^2 , \end{aligned} \quad (16)$$

which involves four coupling constants $l_1, \ldots, l_4$. The quadratic ϕ terms in $L^{(2)}$ describe free mesons of mass m_0. The terms of higher order in ϕ in $L^{(2)}$ and higher order Lagrangians are considered as perturbations.

Inclusion of a finite chemical potential μ related to the electric charge is equivalent to coupling the pions to an external constant electromagnetic vector potential with only temporal component $A_4 = -i\mu$ being nonzero and imaginary. This changes time derivatives in Eqs. (14) and (16) to covariant ones:

$$\partial_\alpha \phi^a \to D_\alpha^{ab}\phi^b = (\partial_\alpha \delta^{ab} - \mu \delta_{\alpha 4}\epsilon^{0ab})\phi^b . \quad (17)$$

This results in the corresponding frequency shifts in the imaginary time propagators of charged pions [10],

$$G_\pm = \frac{1}{(\omega_n \pm i\mu)^2 + \mathbf{p}^2 + m_0^2} , \quad (18)$$

where $\omega_n = 2\pi T n$. It is important that the same shift also occurs in the vertices containing derivatives.

The pressure corresponds to the nonvacuum part of the thermodynamic potential Ω,

$$P(\mu) = \varepsilon_0 - \Omega , \quad (19)$$

$$\Omega = -\lim_{V\to\infty} \frac{T}{V} \ln[\mathrm{Tr}\, e^{-(H-\mu Q)/T}] , \quad (20)$$

where ε_0 is the zero temperature and chemical potential limit of Ω. Thus, to calculate $P(\mu)$ one should consider all closed-loop diagrams involving all possible couplings from $L_{\rm eff}$. We will confine ourselves here to the second order in the density of the pion gas and thus take into account only the diagrams with one and two thermal loops. First we consider the noninteracting pion gas thermodynamic potential $\Omega_\pm^{(0)}$, and pion propagators and their derivatives at the origin:

$$\Omega_\pm^{(0)} = -\int \frac{d^3p}{(2\pi)^3} T \sum_n \ln[\omega^2 + (\omega_n \pm i\mu)^2] , \quad (21)$$

$$G_\pm(0) = \int \frac{d^3p}{(2\pi)^3} T \sum_n \frac{1}{\omega^2 + (\omega_n \pm i\mu)^2} , \quad (22)$$

$$D_0 G_\pm(0) = \int \frac{d^3p}{(2\pi)^3} T \sum_n \frac{i(\omega_n \pm i\mu)}{\omega^2 + (\omega_n \pm i\mu)^2} , \quad (23)$$

and similar expressions for second derivatives. Here $\omega^2 = m_0^2 + \mathbf{p}^2$. Note that a single spatial derivative would give a zero result, and that $D_0 G_\pm(0)$ is zero at $\mu = 0$. These terms with temporal covariant derivatives contribute new terms to $P(\mu)$ which are absent at $\mu = 0$. The corresponding temperature-dependent finite parts of the above expressions are

$$\Omega_\pm^{(0)} \to g_0(\mu) = -T \int \frac{d^3p}{(2\pi)^3} \left[\ln\left(1 - e^{-(\omega+\mu)/T}\right) + \ln\left(1 - e^{-(\omega-\mu)/T}\right)\right] , \quad (24)$$

$$G_{\pm}(0) \to g_1(\mu) = \int \frac{d^3p}{(2\pi)^3}\frac{1}{2\omega}\left[\frac{1}{e^{(\omega+\mu)/T}-1}+\frac{1}{e^{(\omega-\mu)/T}-1}\right], \tag{25}$$

$$D_0 G_{\pm}(0) \to \pm\frac{1}{2}\frac{\partial g_0(\mu)}{\partial\mu} = \pm\int \frac{d^3p}{(2\pi)^3}\left[\frac{1}{e^{(\omega+\mu)/T}-1}-\frac{1}{e^{(\omega-\mu)/T}-1}\right]. \tag{26}$$

We also introduce two combinations of $g_0(\mu)$ and $g_1(\mu)$:

$$g(\mu) = 3g_0^2(\mu) + 3m_\pi^2 g_0(\mu)g_1(\mu), \quad \bar{g}(\mu) = 3g_0(\mu)g_0(0) + \tfrac{3}{2}m_\pi^2\left[g_0(0)g_1(\mu)+g_0(\mu)g_1(0)\right]. \tag{27}$$

To simplify comparisons with the case $\mu = 0$, we follow the notation of Ref. [9] in which the two-loop formula for the pressure contained functions g_0, g_1, and their combination $g = 3(g_0^2 + m_\pi^2 g_0 g_1)$, so that $g_0(0) = g_0$, $g_1(0) = g_1$, and $g(0) = \bar{g}(0) = g$. In terms of $g_0(\mu)$, $g_1(\mu)$, $g(\mu)$, and $\bar{g}(\mu)$ the two-loop pressure at $\mu \neq 0$ takes the form

$$\begin{aligned}
P(\mu) = {} & \frac{1}{2}[g_0 + 2g_0(\mu)] - \frac{m_0^2}{8F^2}\left[4g_1(\mu)g_1(0) - g_1^2(0) + \frac{2}{m_\pi^2}\left(\frac{\partial g_0}{\partial\mu}\right)^2\right] \\
& + \frac{m_0^4}{96\pi^2F^4}(\bar{l}_1+2\bar{l}_2)\left[3g_1^2(0)+4g_1(\mu)g_1(0)+8g_1^2(\mu)\right] - \frac{m_0^4}{64\pi^2F^4}\bar{l}_3\left[g_1^2(0)+2g_1^2(\mu)-\frac{1}{2m_\pi^2}\left(\frac{\partial g_0}{\partial\mu}\right)^2\right] \\
& + \frac{m_0^4}{256\pi^2F^4}\left[13g_1^2(0)+28g_1^2(\mu)+4g_1(\mu)g_1(0)-\frac{5}{m_\pi^2}\left(\frac{\partial g_0}{\partial\mu}\right)^2\right] \\
& + \frac{1}{48\pi^2F^4}\left\{\bar{l}_1\left[g(0)+2g(\mu)\right]+2\bar{l}_2\left[g(0)+3g(\mu)+2\bar{g}(\mu)\right]\right\} - \frac{1}{1152\pi^2F^4}\left[9g(0)+38g(\mu)+40\bar{g}(\mu)\right].
\end{aligned} \tag{28}$$

Here we introduced the renormalized coupling constants [8] $\bar{l}_1, ..., \bar{l}_4$ through the relation

$$l_i = \gamma_i\left(\lambda + \frac{1}{32\pi^2}\bar{l}_i\right), \tag{29}$$

where λ is a logarithmically divergent term and $\gamma_1 = 1/3$, $\gamma_2 = 2/3$, $\gamma_3 = -1/2$, and $\gamma_4 = 2$. We use dimensional regularization since it preserves gauge invariance. We use the mass renormalization relation [8]

$$m_\pi^2 = m_0^2\left(1 - \frac{m_0^2}{32\pi^2F^2}\bar{l}_3\right) \tag{30}$$

so that g_0, g_1, g, and $\bar{g}$ in Eq. (28) are functions of m_π^2.

It is very useful to compare the representation for the pressure $P(\mu)$ obtained with the method of chiral Lagrangians to the result of the virial expansion in Sec. II. It is of course evident that the first term in Eq. (28), which is the ideal gas pressure, is exactly the same as Eq. (10). Using the low temperature expansions of g_0 and g_1,

$$g_0(\mu) = 2\cosh(\mu\beta)\frac{T^{5/2}m_\pi^{3/2}}{(2\pi)^{3/2}}e^{-m_\pi/T}\left(1+\frac{15}{8}\frac{T}{m_\pi}+\cdots\right) + O(e^{-2m_\pi/T}), \tag{31}$$

$$g_1(\mu) = \cosh(\mu\beta)\frac{T^{3/2}m_\pi^{1/2}}{(2\pi)^{3/2}}e^{-m_\pi/T}\left(1+\frac{3}{8}\frac{T}{m_\pi}+\cdots\right) + O(e^{-2m_\pi/T}),$$

in Eq. (28) the pressure may be written as a series:

$$P(\mu) = T(m_\pi T/2\pi)^{3/2}\sum_{n=1}^{\infty}B_n(\mu)\exp(-nm_\pi/T). \tag{32}$$

The $n = 1$ term here is the Boltzmann limit of the free gas pressure, Eq. (10), while the $n = 2$ term contains both $O(e^{-m_\pi/T})$ corrections to this limit and the contribution of the interaction:

$$B_2(\mu) = B_2^{(0)}(\mu) + B_2^{\rm int}(\mu, \bar{l}_i). \tag{33}$$

The case of a relativistic free gas corresponds to

$$B_n(\mu) = B_n^{(0)}(\mu) = [1+2\cosh(\mu\beta)]n^{-5/2} \times\left(1+\frac{15}{8n}\frac{T}{m_\pi}+\cdots\right). \tag{34}$$

On the other hand, one can start from Eq. (9), take the standard low momentum ($q << m_\pi$) representation for the phase shifts,

$$\sin 2\delta_l^I(q) = 2q^{2l+1}(m_\pi^2+q^2)^{-1/2}(a_l^I + q^2 b_l^I + \cdots), \tag{35}$$

and use the scattering lengths and effective radii calculated in the chiral perturbation theory [8] in terms of the couplings $\bar{l}_i$:

$$a_0^0 = \frac{7m_0^2}{32\pi^2F^2}\left[1+\frac{5m_0^2}{84\pi^2F^2}\left(\bar{l}_1+2\bar{l}_2-\frac{9}{10}\bar{l}_3+\frac{21}{8}\right)+O(m_0^4)\right],$$
$$a_0^2 = -\frac{m_0^2}{16\pi^2F^2}\left[1-\frac{m_0^2}{12\pi^2F^2}\left(\bar{l}_1+2\bar{l}_2+\frac{3}{8}\right)+O(m_0^4)\right],$$
$$b_0^0 = \frac{1}{4\pi F^2}\left[1+\frac{m_0^2}{12\pi^2F^2}\left(2\bar{l}_1+3\bar{l}_2-\frac{13}{16}\right)+O(m_0^4)\right],$$
$$b_0^2 = -\frac{1}{8\pi F^2}\left[1-\frac{m_0^2}{12\pi^2F^2}\left(\bar{l}_1+3\bar{l}_2-\frac{5}{16}\right)+O(m_0^4)\right],$$
$$a_1^1 = \frac{1}{24\pi F^2}\left[1-\frac{m_0^2}{12\pi^2F^2}\left(\bar{l}_1-\bar{l}_2+\frac{65}{48}\right)+O(m_0^4)\right]. \quad (36)$$

A straightforward check shows that the contributions of interaction to the pressure agree in the two approaches and $B_2^{\rm int}(\mu,\bar{l}_i)$ may be written as

$$B_2^{\rm int}(\mu) = \left(\frac{2T}{\pi m_\pi}\right)^{1/2}\left[a(\mu)+\frac{3T}{2m_\pi}\left[\frac{1}{2}a(\mu)+m_\pi^2 b(\mu)\right]+O\left(\frac{T^2}{m_\pi^2}\right)\right], \quad (37)$$

where

$$a(\mu) = 2\cosh(2\mu\beta)\,a_0^2+2\cosh(\mu\beta)\,a_0^2+a_0^2+a_0^0,$$
$$b(\mu) = 2\cosh(2\mu\beta)\,b_0^2+2\cosh(\mu\beta)\,(b_0^2+3a_1^1)+b_0^2+b_0^0+3a_1^1. \quad (38)$$

At $\mu = 0$ this coincides with the result obtained in Ref. [9]. It should be noted that the $(\partial g_0/\partial\mu)^2$ terms in Eq. (28) for the pressure are proportional to $\sinh^2(\mu\beta)$. They are absent at $\mu = 0$ and crucial for agreement with the virial result.

The screening mass is finally obtained from Eq. (28) using Eq. (1):

$$m_{\rm el}^2 = g_0''(0)-\frac{m_\pi^2}{2F^2}\left(g_1''(0)g_1(0)+\frac{[g_0''(0)]^2}{m_\pi^2}\right)+\frac{5m_\pi^4}{24\pi^2F^4}\left[\left(\bar{l}_1+2\bar{l}_2-\frac{3}{8}\bar{l}_3+\frac{9}{8}\right)g_1''(0)g_1(0)-\frac{3}{16}\frac{[g_0''(0)]^2}{m_\pi^2}+\left(\bar{l}_1+4\bar{l}_2-\frac{29}{24}\right)\frac{g''(0)}{5m_\pi^4}\right], \quad (39)$$

where $g_i''(0) \equiv \partial^2 g_i/\partial\mu^2(\mu=0)$. Odd derivatives of g_i with respect to μ are zero at $\mu = 0$. Here we eliminated m_0 in favor of the physical pion mass m_π. The first term is of course exactly the same as in Eq. (11). All other terms are due to the interaction. One can check, as in the case of pressure, that they coincide to relative order $(T/m_\pi)^{3/2}$ with what follows from the interaction part of the virial result in Eq. (11) if the approximation of effective radius is used for the phase shifts.

In numerical calculation we use the central values of the recent estimates of the couplings $\bar{l}_i$ obtained in Ref. [11]:

$$\bar{l}_1 = -0.62\pm0.94, \quad \bar{l}_2 = 6.28\pm0.48,$$
$$\bar{l}_3 = 2.9\pm2.4, \quad \bar{l}_4 = 4.3\pm0.9 \quad (40)$$

(the coupling $\bar{l}_4$ relates $F \approx 87$ MeV to the physical coupling $F_\pi = 93$ MeV [8]). The results of this calculation are presented in Fig. 3. The dashed curve represents noninteracting pions. The chain-dashed curve includes the contributions of interactions to order F^{-2}, and the solid curve includes also the contributions of order F^{-4}. We have displayed these separately because the chiral perturbation theory is naturally expressed as an expansion in inverse powers of F. See Eqs. (28) and (39). There is reasonable agreement with the virial calculation up to temperatures of around 80 MeV. Above 100 MeV the chiral perturbation expansion does not seem convergent. The order F^{-4} result starts to blow-up. This can be traced to the basic derivative expansion of the Lagrangian. For example, the low momentum expansion of the phase shifts in Eq. (35) will be inadequate because the average two-pion collision energy grows with temperature.

It should be noted that in obtaining Eqs. (28) and (39) we have actually taken into account three-loop diagrams which contain up to two thermal loops. Because of these thermal loops the final results are quadratic in the phase space functions g_0 and g_1. The third, $T = 0$ loop, is responsible for the renormalization of the couplings l_i. There is, however, one three-loop diagram which does not factorize into $T = 0$ and $T \neq 0$ loops. This is the eye-type diagram and we did not take it into account. As was shown in [9] it gives a contribution to the pressure which is proportional to $\exp(-m_\pi/T)$, but is suppressed by an additional preexponential factor of T/m_π. It contributes to the $O(T^2/m_\pi^2)$ term in Eq. (37) and thus is related to q^4 terms in the expansion equation (35). This contribution should become important at $T \sim m_\pi$ which explains the deviation from the virial result which uses experimental information on phase shifts.

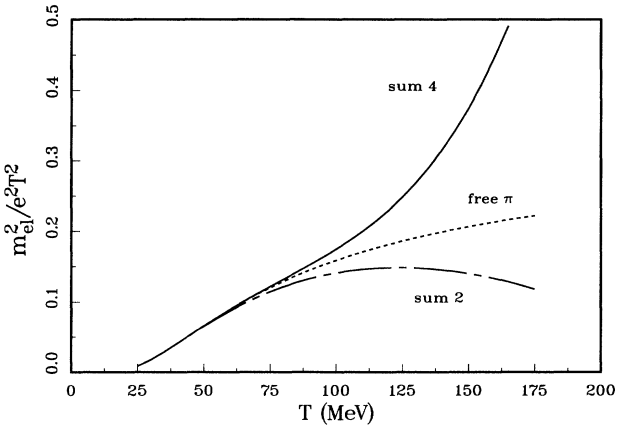

FIG. 3. Same as Fig. 2 but from chiral perturbation theory. The dashed line represents free pions. The chain-dashed line includes the effects of interactions to order F^{-2}. The solid line includes the effects of interactions to order F^{-4}.

IV. FREE BOSONS ON A LATTICE

In principle Monte Carlo simulations of lattice QCD should predict the properties of strongly interacting matter at all temperatures, including the low temperature phase of hadrons. So far little has been learned about the low temperature phase due to limitations of finite lattice size and lattice spacing and the difficulty of doing calculations with light quarks. Some years ago, singlet and nonsinglet quark number susceptibilities were computed on a lattice of size $8^3 \times 4$ [12]. These susceptibilites are linear combinations of the baryon and electric susceptibilities. The latter is just the square of the electric screening mass up to a factor of e^2. Since then calculations have also been done on a $10^3 \times 6$ lattice [13] and these were used in Ref. [1]. See Fig. 1. The temperature range covered by this larger lattice is about 120 to 190 MeV, which is just in the interesting regime where a crossover from hadron to quark-gluon degrees of freedom takes place. When comparing the results of lattice QCD with continuum field theory calculations it is important to have an estimate of how important finite lattice size and spacing effects are. This is true not only of the lattices just mentioned, but also for lattices to be used in the upcoming Teraflop project; typical lattices are expected to be 48^3. Is this large enough?

To get a handle on this question we consider a system of noninteracting, massive, charged scalar bosons on a lattice at finite temperature and chemical potential. Fermions with a chemical potential have been studied on the lattice [14,15] but apparently there are no reports of the boson calculation in the literature. Since this is a free theory, the partition function can be evaluated exactly, and from this one can compute the net charge (or number) density and the electric susceptibility.

We follow here the notation of Creutz [16]. We consider a Euclidean lattice of size $N_s^3 \times N_t$ with equal lattice spacing a in the space and time directions. Roman indices run from 1 to 3, Greek indices run from 1 to 4, with 4 being the time direction. A lattice site is specified by $x_\nu = a n_\nu$. The integers n have allowed values

$$-\frac{N_s}{2} < n_i \le \frac{N_s}{2}, \qquad -\frac{N_t}{2} < n_4 \le \frac{N_t}{2}. \tag{41}$$

The temperature is $T = 1/N_t a$ and the physical length of a side of the three-dimensional cube is $L = 1/N_s a$. Letting Φ denote the complex scalar field, the action is

$$S = a^4 \sum_{(l,n)} \left[\frac{\Phi^*(l) - \Phi^*(n)}{a}\right]\left[\frac{\Phi(l) - \Phi(n)}{a}\right] + m^2 a^4 \sum_n \Phi^*(n)\Phi(n), \tag{42}$$

where the first sum is over all nearest neighbors (l,n). We shall impose periodic boundary conditions in the spatial directions, and of course finite temperature requires the fields to be periodic in the time direction.

We introduce a chemical potential corresponding to the conserved charge in the same way as one normally introduces an electromagnetic vector potential [14]. That is, we make the replacement $iA_4 \to iA_4 + \mu$. This ensures that the chemical potential couples to exactly the same charge density as the time component of the vector potential. This maintains gauge invariance. Thus, in the action, the only term which changes is

$$-a^2 \sum_n \Big[\Phi^*(\mathbf{n}, n_4 + 1) e^{a\mu} \Phi(\mathbf{n}, n_4) + \Phi^*(\mathbf{n}, n_4) e^{-a\mu} \Phi(\mathbf{n}, n_4 + 1)\Big]. \tag{43}$$

We can think of this as giving particles (going forward in time) a chemical potential μ and antiparticles (going backward in time) a chemical potential $-\mu$. This is usually called a link hopping term.

In order to carry out the functional integration over the fields it is convenient to express them in terms of their Fourier components.

$$\Phi(n) = \frac{1}{N_s^3 N_t} \sum_k \tilde{\Phi}(k) \exp\left[-2\pi i \left(\frac{\mathbf{k}\cdot\mathbf{n}}{N_s} + \frac{k_4 n_4}{N_t}\right)\right], \tag{44}$$

where the components of the vector k are allowed the same values as the components of the vector n. Inserting this Fourier decomposition into the expression for the action, integrating over the lattice sites with the help of

$$\frac{1}{N_s^3 N_t} \sum_n \exp\left[2\pi i \left(\frac{\mathbf{k}\cdot\mathbf{n}}{N_s} + \frac{k_4 n_4}{N_t}\right)\right] = \delta_{k_\nu, 0}, \tag{45}$$

we get the action in the form

$$S = \frac{1}{2} \frac{a^4}{N_s^3 N_t} \sum_k D(k) \left[\tilde{\phi}_1^2(k) + \tilde{\phi}_2^2(k)\right], \tag{46}$$

where $\Phi = (\phi_1 + i\phi_2)/\sqrt{2}$ and the propagator is

$$D(k) = m^2 + \frac{2}{a^2} \sum_i \left[1 - \cos\left(\frac{2\pi k_i}{N_s}\right)\right] + \frac{2}{a^2}\left[1 - \frac{1}{2}\left(\exp\left\{a\mu + \frac{2\pi i k_4}{N_t}\right\} + \exp\left\{-a\mu - \frac{2\pi i k_4}{N_t}\right\}\right)\right]. \tag{47}$$

The logarithm of the partition function is, up to an irrelevant additive constant, given by

$$\ln Z = \ln \int [d\Phi] e^{-S} = -\ln \det\left[a^2 D(k)\right]. \tag{48}$$

Let us define a relativistic lattice energy ϵ by

$$\epsilon^2 = m^2 + \frac{4}{a^2} \sum_i \sin^2\left(\frac{\pi k_i}{N_s}\right). \tag{49}$$

Let us also define the complex variable

$$z = \exp\left\{\frac{2\pi i k_4}{N_t}\right\}. \tag{50}$$

Then the partition function can be expressed as

$$\ln Z = -\sum_k \ln\left[2 + a^2\epsilon^2 - ze^{a\mu} - z^{-1}e^{-a\mu}\right] . \quad (51)$$

It is expedient to differentiate with respect to the chemical potential before doing the summations. This gives the net particle number (or charge) of the system:

$$N = T\frac{\partial \ln Z}{\partial \mu} = aT\sum_k \frac{ze^{a\mu} - z^{-1}e^{-a\mu}}{2 + a^2\epsilon^2 - ze^{a\mu} - z^{-1}e^{-a\mu}} . \quad (52)$$

We now perform the sum over k_4 analytically with the help of the formula

$$\sum_{k_4} f\left(e^{\frac{2\pi i k_4}{N_t}}\right) = \frac{N_t}{2\pi i}\int_C \frac{dz}{z}\frac{f(z)}{z^{N_t} - 1} , \quad (53)$$

where C is any closed contour containing the points satisfying $z^{N_t} = 1$ and which does not include the origin $z = 0$. Thus

$$N = \sum_{\mathbf{k}} \frac{1}{2\pi i}\int_C \frac{dz}{z}\frac{f(z)}{z^{N_t} - 1} , \quad (54)$$

where

$$f(z) = \frac{ze^{a\mu} - z^{-1}e^{-a\mu}}{2 + a^2\epsilon^2 - ze^{a\mu} - z^{-1}e^{-a\mu}} . \quad (55)$$

The function f has simple poles at $z = \exp[a(\pm\omega - \mu)]$ where $\omega > 0$ is defined by

$$\sinh\left(\frac{a\omega}{2}\right) = \frac{a\epsilon}{2} . \quad (56)$$

If one analytically continues from Euclidean space (imaginary time) to Minkowski space (real time), as is appropriate for obtaining a response function, then the Matsubara frequency $2\pi k_4 Ti \to p_0$, where p_0 is a real, continuous energy. The single-particle energies are determined by the poles of the propagator. In the limit of a vanishing chemical potential these poles are located at $p_0 = \pm\omega$ where ω is as defined in the equation above. With some rearrangement we can replace the integral over the single closed contour C with integrals over three disjoint contours C_+, C_- and C_0 encircling the two poles of $f(z)$ and the origin. The residues are easily evaluated. Dividing by the volume we obtain the number density:

$$n = \frac{1}{(N_s a)^3}\sum_{\mathbf{k}}\left[\frac{1}{e^{(\omega-\mu)/T} - 1} - \frac{1}{e^{(\omega+\mu)/T} - 1}\right] . \quad (57)$$

This is a familiar form. It is now easy to integrate n with respect to μ to obtain the partition function:

$$\ln Z = -\sum_{\mathbf{k}}\left[\ln\left(1 - e^{-(\omega-\mu)/T}\right) + \ln\left(1 - e^{-(\omega+\mu)/T}\right)\right] . \quad (58)$$

In the continuum theory Bose-Einstein condensation occurs when the chemical potential approaches the mass. On the lattice the condition is slightly modified. The number density diverges as μ approaches the critical value determined from

$$\sinh\left(\frac{a\mu_{\rm crit}}{2}\right) = \frac{am}{2} . \quad (59)$$

This allows for any finite number of particles on the lattice even when the temperature goes to zero. In that limit, all particles are concentrated in the zero momentum mode.

Both the partition function and the number density vanish in the zero temperature limit ($N_t \to \infty$ at fixed a) so long as $-\mu_{\rm crit} < \mu < \mu_{\rm crit}$. They both have the correct limits as the continuum is approached: $a \to 0$, $N_t \to \infty$, $N_s \to \infty$ with $N_t \ll N_s$, and $T = 1/N_t a$ fixed.

Now we turn to the electric susceptibility. Differentiating n with respect to μ, and setting $\mu = 0$, we get

$$\frac{\partial n}{\partial \mu}(\text{lattice}) = 2\left(\frac{N_t}{N_s}\right)^3 T^2\sum_{\mathbf{k}}\frac{e^{\omega/T}}{\left(e^{\omega/T} - 1\right)^2} . \quad (60)$$

This reproduces the correct expression in the continuum limit:

$$\frac{\partial n}{\partial \mu}(\text{continuum}) = \frac{2}{T}\int\frac{d^3p}{(2\pi)^3}\frac{e^{\omega/T}}{\left(e^{\omega/T} - 1\right)^2} , \quad (61)$$

where here $\omega = \sqrt{m^2 + \mathbf{p}^2}$. The ratio of these two expressions, lattice/continuum, depends only on the single dimensionless variable T/m for a given lattice $N_s^3 \times N_t$, since the lattice spacing can be written as $a = 1/N_t T$.

In Fig. 4 we plot lattice/continuum for lattices of size $8^3 \times 4$ and $10^3 \times 6$ for which lattice QCD calculations have been done [12,13]. (We recall that in the QCD calculations the scale is set in such a way that the ρ meson mass has its physical value. The pion is then too heavy, being about 1/2 the ρ mass even for the larger of the two lattices.) The susceptibility on the $10^3 \times 6$ lattice gets to within 40% of the continuum value when $T/m = 0.35$. It deviates markedly for both lower and higher temperatures. As we shall now discuss, the deviation at low

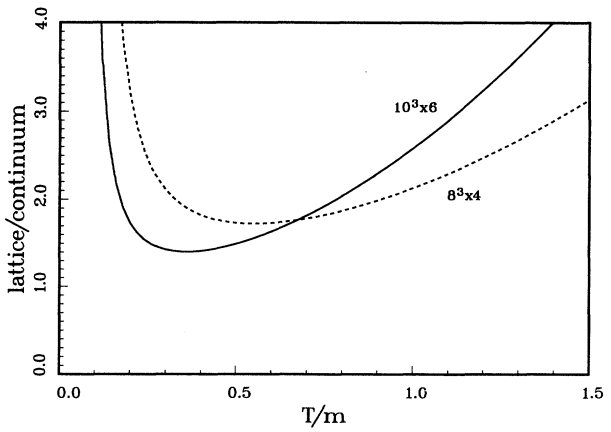

FIG. 4. Ratio of $\partial n/\partial\mu$ on the lattice of specified size to the continuum as a function of temperature over mass.

temperature is caused by finite lattice spacing, while the deviation at high temperature is caused by finite lattice volume.

Apart from the conditions already mentioned which must be satisfied if the lattice is to approximate the continuum, we have another. The lattice spacing must be small compared to all physical length scales. Thus one must have $a \ll 1/m$. This is equivalent to the condition $1/N_t \ll T/m$. Therefore the departure of the lattice susceptibility from the continuum limit will be greater and greater as the temperature gets smaller. This is seen in the figure. From the expressions given above we can readily evaluate the susceptibilities in the low temperature limit:

$$\frac{\partial n}{\partial \mu}(\text{lattice}) \to 2N_t^5 \frac{T^4}{m^2},$$

$$\frac{\partial n}{\partial \mu}(\text{continuum}) \to \frac{1}{4T}\left(\frac{2mT}{\pi}\right)^{3/2} e^{-m/T},$$

$$\text{lattice/continuum} = (2\pi)^{3/2} N_t^5 \left(\frac{T}{m}\right)^{7/2} e^{m/T}. \quad (62)$$

The ratio diverges exponentially as $T/m \to 0$. To get accurate results we obviously cannot go too low in T/m for a fixed value of N_t.

The high temperature limit is equivalent to letting the mass go to zero. The susceptibility of the lattice diverges as the mass vanishes because of the zero momentum mode. This is not true of the susceptibility in the continuum; in the continuum the integral is convergent in the infrared because of the factor $p^2 dp$. Therefore the lattice/continuum ratio also increases at large values of T/m. However, this is a finite lattice volume effect, not finite lattice spacing effect. We can see it in the following ways. If we consider a box of volume L^3 instead of the continuum limit then we would make the replacement

$$\int \frac{d^3p}{(2\pi)^3} \to \frac{1}{L^3}\sum_{\mathbf{p}}. \quad (63)$$

Then the susceptibility diverges in the zero mass limit because of the $\mathbf{p} = \mathbf{0}$ mode, which was suppressed in the integral. Numerically we can see this if we increase the ratio N_t/N_s. To approach the zero lattice spacing, infinite volume, limit we require (among other conditions) that this ratio be small in order that many thermal wavelengths fit within the box. That is, $1/T \ll L$. In this sense the lattice $8^3 \times 4$ is 'bigger' than the lattice $10^3 \times 6$, as is apparent in Fig. 4.

In Fig. 5 we plot the lattice/continuum ratio for lattices of size 48^3 by 12, 16, and 24. These may be typical for the upcoming Teraflop project. On the whole the susceptibilities are much closer to the continuum values than was true for the smaller lattices. However, the small and large T/m behaviors are still apparent, as discussed above. The condition $1 \ll N_t \ll N_s$ is also apparent in the figure.

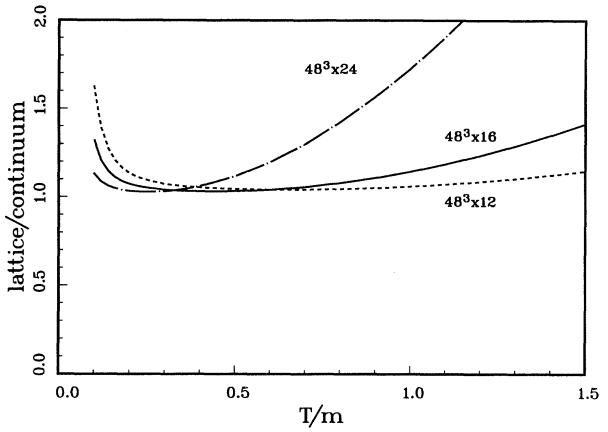

FIG. 5. Ratio of $\partial n/\partial \mu$ on the lattice of specified size to the continuum as a function of temperature over mass.

Since hadrons with masses in the range of 140 to 1000 MeV and beyond are important for the electric screening mass in the temperature range of 50 to 170 MeV or so, it is clear that very large lattices are required to at least reproduce the noninteracting gas results. Whether interaction effects, and the composite nature of the hadrons, are more or less sensitive to finite lattice spacing and volume is not known. It is known, and obvious, that any interaction effects that get big contributions from long wavelength modes are even more sensitive to finite lattice volume [17].

V. CONCLUSION

To get insight into the nature of the expected phase transition (or rapid crossover) of hot hadronic matter to quark-gluon plasma, it is instructive to investigate the temperature dependence of different quantities characterizing the system on both sides of the transition point (or crossover region). We have considered here one such quantity, the electric screening mass, in the case of hadronic gas. We used two different methods: relativistic virial expansion and chiral perturbation theory. They give very similar results up to $T \sim 80$ MeV. At high temperature the applicability of both approaches become doubtful, for somewhat different reasons. In the virial expansion, multipion interactions would have to be taken into account. This is difficult to do theoretically, apart from the fact that multipion scattering amplitudes are practically impossible to obtain experimentally. The advantage of the chiral perturbation expansion is that it very generally takes into account the basic symmetries of QCD in an expansion in powers of the pion mass and space-time derivatives. This is also its limitation. The ρ meson cannot be generated in any finite order; it can arise only from an infinite series of derivative terms in the effective Lagrangian. As the temperature rises, the average relative energy in hadron collisions also rises. Therefore, more and more derivative terms in the expansion must be kept. Not only is this difficult to do theoretically, but the coefficients of the higher order terms are not known yet

from phenomenology. The application of chiral perturbation theory, at least in its present form, is also limited to temperatures below the pion mass.

Numerical simulations on the lattice provide a straightforward possibility to go all the way from low to high temperatures. However, this approach has intrinsic problems due to finite lattice spacing and lattice volume effects. We have shown here that to reproduce the free gas results for the screening mass would require very large lattices. Analytic methods, such as the chiral perturbation theory and the virial expansion, should be useful to obtain estimates on the magnitude of the final volume effects for the interacting hadron gas [18].

ACKNOWLEDGMENTS

We would like to thank H. Leutwyler, L. McLerran, and M. Stone for helpful conversations. This work was supported by the Schweizerischer Nationalfonds, by the Minnesota Supercomputer Institute, and by the U.S. Department of Energy under Grant No. DOE/DE-FG02-87ER40328.

[1] J. I. Kapusta, Phys. Rev. D **46**, 4749 (1992).
[2] E. V. Shuryak, Rev. Mod. Phys. **65**, 1 (1993).
[3] E. V. Shuryak, Nucl. Phys. **A533**, 761 (1991).
[4] G. Welke, R. Venugopalan, and M. Prakash, Phys. Lett. B **245**, 137 (1990).
[5] R. Venugopalan and M. Prakash, Nucl. Phys. **A546**, 718 (1992).
[6] R. Dashen, S-K. Ma, and J. Bernstein, Phys. Rev. **187**, 345 (1969).
[7] S. Weinberg, Phys. Rev. **166**, 1568 (1968); Physica **A96**, 327 (1979).
[8] J. Gasser and H. Leutwyler, Ann. Phys. (N.Y.) **158**, 142 (1984).
[9] P. Gerber and H. Leutwyler, Nucl. Phys. **B321**, 387 (1989).
[10] J. I. Kapusta, *Finite Temperature Field Theory* (Cambridge University Press, Cambridge, England 1989).
[11] C. Riggenbach, J. F. Donoghue, J. Gasser, and B. Holstein, Phys. Rev. D **43**, 127 (1991).
[12] S. Gottlieb, W. Liu, D. Toussaint, R. L. Renken, and R. L. Sugar, Phys. Rev. Lett. **59**, 2247 (1987); S. Gottlieb, W. Liu, R. L. Renken, R. L. Sugar, and D. Toussaint, Phys. Rev. D **38**, 2888 (1988).
[13] R. L. Sugar and D. Toussaint (private communication).
[14] R. V. Gavai and A. Ostendorf, Phys. Lett. **132B**, 137 (1983); J. Kogut, H. Matsuoka, M. Stone, H. W. Wyld, S. Shenker, J. Shigemitsu, and D. K. Sinclair, Nucl. Phys. **B225**, 93 (1983).
[15] H. Matsuoka and M. Stone, Phys. Lett. **136B**, 204 (1984).
[16] M. Creutz, *Quarks, Gluons and Lattices* (Cambridge University Press, Cambridge, England, 1983).
[17] H.-Th. Elze, K. Kajantie, and J. Kapusta, Nucl. Phys. **B304**, 832 (1988).
[18] F. C. Hansen and H. Leutwyler, Nucl. Phys. **B350**, 301 (1991); V. L. Eletsky and M. I. Polikarpov, in *Effective Field Theories of the Standard Model*, edited by Ulf-G. Meissner (World Scientific, Singapore, 1992).